

Advanced Lighting for Unstructured-Grid Data Visualization

Category: Research

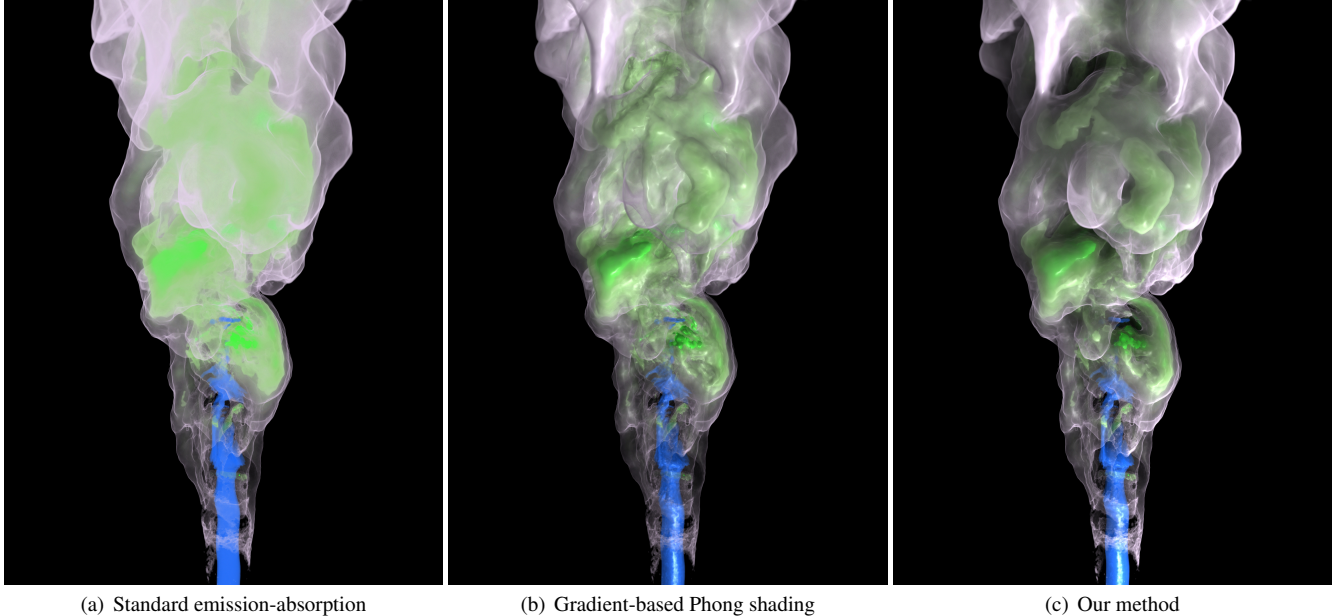


Figure 1: Unstructured grid volume visualization examples showing advantages using our method. The H_2O field of the Flame dataset is visualized. With our method, shadows enhance the visual perception of depth cue largely.

ABSTRACT

The clear benefits of using advanced illumination models in volume visualization have been demonstrated by many researchers. Interactive volume rendering incorporated with advanced lighting has been achieved with GPU acceleration for regular-grid volume data, making volume visualization even more appealing as a tool for 3D data exploration. This paper presents an interactive illumination strategy, which is specially designed and optimized for volume visualization of unstructured-grid data. The basis of the design is a partial differential equation based illumination model to simulate the light propagation, absorption, and scattering within the volumetric medium. In particular, a novel numerical scheme is introduced to overcome the challenges presented by unstructured grids. Test results show that the added illumination effects such as global shadowing and multiple scattering not only lead to more visually pleasing visualization, but also greatly enhance the perception of the depth information and complex spatial relationships for features of interest in the volume data. This volume visualization enhancement is timely with the growing use of unstructured grids in a variety of scientific simulation applications.

Index Terms: I.3.7 [Computer Graphics]: Three-Dimensional Graphics and Realism—Color, shading, shadowing, and texture; I.3.8 [Computer Graphics]: Applications

1 INTRODUCTION

Direct volume rendering (DVR) is widely used to examine 3D field data in the area of scientific visualization. For effective visualization, an important aspect of volume rendering is the ability to provide visual cues to aid users in comprehending the spatial structures in the datasets. Although simple Phong shading is

fast, it is mainly computed with an approximation of local surface orientations, which gives limited realism and may introduce unwanted surface details. On the other hand, advanced illumination models that provide global lighting effects such as global shadows and multiple scattering can greatly enhance depth cues and better present the local thickness of layer features in the data, leading to better imagery results for depicting complex volumetric features. Another key aspect of volume rendering is interactivity. Thanks to the enormous processing power provided by modern graphics hardware, volume rendering can be performed in real-time today. Several techniques to apply visually plausible global illumination effects to volume rendering at interactive speed have been introduced [1] [11] [13] [14] [18] [21] [26].

However, most of interactive illumination techniques utilize the graphics hardware's ability to accelerate computing on regular rectilinear grids of volume elements. Volume rendering with high quality illumination of data that come in other forms of geometry such as warped grids or unstructured grids that are widely used in scientific simulations is still a challenge. The main difficulties we encountered in dealing with unstructured grids are

- the non-uniform distribution of the vertices,
- the high cost of sampling arbitrary point in the volume domain, and
- the non-convexity of the volume grid.

Unlike regular grids, the vertices in an unstructured grid are distributed unevenly, often clustered in a small area of the volume domain in order to provide high resolution on interesting regions of the dataset. Therefore, most of texture-based techniques are not

appropriate to be used because they cannot provide required resolution adaptability and may loss accuracy for finer cells in the grid. Also, the acceleration techniques relying on the regularity of the data such as summed area tables (SAT) are not capable of handling unstructured grids. Sampling arbitrary point in a unstructured grid is an expensive operation because it usually involves in a search process within a spatial data structure to locate the point. The non-convexity of the volume grid may cause problems when simulating light transport. The cases that light goes out from the volume and then goes into the volume again must be carefully considered or else the results would be incorrect.

In this paper, we present a method for interactive volume rendering of unstructured-grid data with high quality illumination including shadowing and multiple scattering effects. The method is based on a partial differential equation (PDE) based illumination model [26]. Addressing aforementioned challenges presented by unstructured grids, our contribution are mainly as follows: (i) A two-level approach which not only solves the non-convexity problem but also accelerates the computation. (ii) The derivation of the numerical scheme to solve the model equation on unstructured grids. In particular, in order to achieve numerical stability and high efficiency, a semi-Lagrangian scheme is used. Our method can be easily generalized to handle other types of grids including curvilinear, AMR, and even hybrid grids. Furthermore, since the method is not hardly depend on preprocessing, it is even suitable for time-varying data.

2 RELATED WORK

The volume illumination involves solving the radiative transfer equation [3], which formalizes the evolution of light transport with participating media, including light absorption, scattering and emission effects. Max [17] presented an overview on the optical models used in direct volume rendering (DVR). Kajiya and von Herzen [12] presented a model for rendering volume densities which included multiple scattering computation. The scattering equation is solvable analytically only in some simple configurations. Several methods have been proposed to numerically solve the radiative transfer equation by using either ray tracing [15] [16] or radiosity [20]. These methods are capable of rendering various illumination effects with arbitrary phase functions and heterogeneous media. However, the computational cost is tremendous, and the speed is far from the requirement of interaction.

To simulate light transport in participating media, Jensen and Christensen proposed a two-pass method using volumetric photon mapping (VPM) [10]. In its first stage, the method traces photons throughout the volume and stores them into spatial hierarchical data structure. In the second pass, an adaptive ray marching algorithm is used and the pre-stored photons are gathered for final radiance. There are many methods aiming to improve the efficiency of VPM [2] [8]. However, the cost of creation and maintenance of the hierarchical structure prevents early VPM methods from achieving interactive performance. More recently, Jönsson et al. [11] presented an interactive method extending photon mapping. By tracking the history of photons, full recomputation of the photon map can be avoided when the transfer function is changed; instead, only the photons affected by the parameter changes are recomputed. However, full recomputation is still required when the parameter change affects all photons such as moving light source or when time-varying data is visualized. However, in the context of unstructured-grid DVR, photon mapping based methods may suffer from the adaptive nature of the unstructured grids. Large amount of photons may needed in order to fulfill the accuracy requirement in the high resolution regions of the grid.

Many interactive techniques have been proposed to enhance the volume rendering for visualization by supporting illumination effects such as shadowing and scattering. For example, obscurance

and ambient occlusion (AO) methods provide relatively inexpensive ways to approximate indirect illumination. GPU-based screen space ambient occlusion (SSAO) [23] is a high-performance technique to render occlusion effects in polygonal shading by sampling the depth buffer in screen space. It can also be applied to volume rendering [7]. Although efficient, SSAO may not produce desired results in complex scenarios, for example, semitransparent objects, since only one depth value per pixel can be used. Object space AO, as shown in the paper of Ruiz et al. [19], provides better quality while the memory and computation cost is higher than SSAO. The evaluation of occlusion/extinction can be accelerated through the use of SAT [7] [21], but the SAT based techniques cannot be used for unstructured grids. Recently, Schott et al. [22] demonstrated an ambient occlusion technique for interactive volume rendering that can render mutual occlusion effects of both volume and geometric primitives, which is also supported by our method.

Although multiple scattering is important for realistic rendering of participating media, Max has stated that it is overkill to compute it in most scientific visualization applications [17]. However, it has been shown that physically plausible approximation to the global illumination effects can improve perceptual quality of the visualization [18]. Kniss et al. [13] [14] proposed an interactive shading model that incorporated volumetric shadows and scattering effects, where scattering is restricted to forward scattering and estimated by applying blurring operations within a cone toward the light source. Using half-angle slicing, the lighting can be evaluated efficiently in the image space, but the light configuration is limited to a single light source. Extending the idea of Kniss et al., Ropinski et al. [18] applied the lighting computation directly in volume space. In their approach, the light volume is computed first, where the light propagation is evaluated slice by slice, and then used in the shading stage of rendering. Thus, the method is applicable to any volume rendering technique, including GPU-based ray casting. However, in the context of unstructured-grid DVR, the uniform slices may not be able to provide sufficient resolution in some regions of the volume since the mesh can be highly adaptive. Following the cone-sampling idea presented by Kniss et al., Schlegel et al. [21] approximated the soft shadows and scattering effects by aggregating the extinction values within the shadow cone. In their approach, the cone is approximated by a series of cuboids, and the extinction computation of the cuboids is accelerated by employing SAT. Ament et al. [1] presented a pre-integration method for scattering in DVR, which also utilizes SAT for fast extinction values summation. The pre-integration table, independent of dataset and transfer function, is obtained by solving the full light transport with a Monte-Carlo simulation within a set of spherical regions. By employing SAT, the ambient extinction coefficient, one of the parameters of the table, can be efficiently computed, enabling interactive volume rendering. However, SAT do not work for unstructured data, and therefore the evaluation of the extinction values can be expensive in unstructured-grid DVR.

As mentioned already, the grid-based volume illumination method presented by Zhang and Ma [26] built the foundation of our work. We extend their method by supporting unstructured grids. Although gradient-based local Phong lighting has been used to help understand spatial structures of unstructured-grid data [6], to our knowledge, very few papers address on interactive global illumination for unstructured grid volume rendering.

3 ILLUMINATION MODEL

Zhang and Ma [26] proposed a two-step, PDE-based illumination model for interactive volume rendering, which uses a single value to encode light energy at each spatial location for each light source. The light propagation, absorption and scattering are modeled as a

convection-diffusion equation

$$\frac{\partial}{\partial t} \rho(\mathbf{x}) = -c\mathbf{u}(\mathbf{x}) \cdot \nabla \rho(\mathbf{x}) - \sigma_a(\mathbf{x})\rho(\mathbf{x}) + \sigma_s \nabla^2 \rho(\mathbf{x}) \quad (1)$$

where $\rho(\mathbf{x})$ is the energy density at \mathbf{x} , c is the speed of light, $\mathbf{u}(\mathbf{x})$ is the unit light propagation direction at \mathbf{x} , $0 \leq \sigma_a(\mathbf{x}) \leq 1$ is the absorption coefficient at \mathbf{x} , and σ_s is the isotropic scattering coefficient. The solution of $\rho(\mathbf{x})$ of each light source is combined into a single light color field by

$$L(\mathbf{x}) = \sum_{k=1}^N \rho_k(\mathbf{x}) L_k \quad (2)$$

where L_k is the color of the k th light source. The light color field value L is used to shade the sample points in the rendering process. In order to exhibit the surface shape, the light value can be used with gradient-based Phong shading

$$L_{final}(\mathbf{x}) = L(\mathbf{x})(I_a(\mathbf{x}) + I_d(\mathbf{x}) + I_s(\mathbf{x})) \quad (3)$$

where I_a , I_d , and I_s are the ambient term, diffuse term, and specular term of Phong lighting, respectively.

To reduce computational cost, Eq. 1 can be split into a convection equation

$$\frac{\partial}{\partial t} \rho(\mathbf{x}) = -c\mathbf{u}(\mathbf{x}) \cdot \nabla \rho(\mathbf{x}) - \sigma_a(\mathbf{x})\rho(\mathbf{x}), \quad (4)$$

which needs to be evaluated for each light source, and a diffusion equation

$$\frac{\partial}{\partial t} \rho(\mathbf{x}) = \sigma_s \nabla^2 \rho(\mathbf{x}) \quad (5)$$

which is independent of light sources and needs to be solved only once for multiple light sources.

Zhang and Ma [26] showed a regular grid-based numerical solver for the illumination model. We follow this framework and extend the method for unstructured-grid data.

4 LIGHT VOLUME CALCULATION

In this section we show how we solve Eq. 1 for unstructured grids.

A simple approach to apply the illumination method described in the previous section to an unstructured grid is to resample the data onto a regular grid for light simulation. However, since an unstructured grid can be highly adaptive, the vertices of the grid may be distributed unevenly and clustered in a small area of the volume domain. Thus, the light field evaluated according to the resampled volume may not be able to provide sufficient accuracy for the regions with originally finer cells. To best fit the accuracy requirement, the volume domain should be discretized according to the original unstructured grid for light simulation.

However, a significant issue of simulating light on unstructured grids is the handling of non-convex meshes. When ray casting non-convex meshes, the concaves and holes in the mesh may cause re-entry problem. Our light field evaluation process suffers from a similar problem; since the light cannot be propagated across the concaves and holes, the light propagation may be evaluated incorrectly as shown in Figure 2 (a), and the boundary conditions are hard to be determined at the concaves and holes.

We solve the problem by introducing a two-level approach, where the first level is a resampled Catesian grid (henceforth referred to as *level-0* grid), and the second level is the original unstructured grid (henceforth referred to as *level-1* grid). To calculate the light field values, we first simulate the light propagation on the level-0 grid, so that the light can propagate across concaves and holes. Then the solution on the level-0 grid is interpolated into level-1 grid as Dirichlet boundary values and initial values. Then

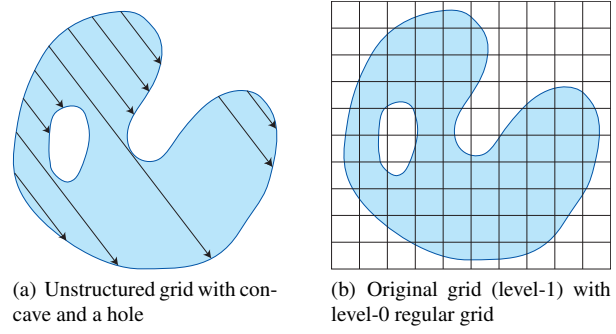


Figure 2: (a) Assuming that the space in the concaves and holes is transparent, the light should be propagated across the concaves and holes. If this situation does not handled properly, the simulation result will be incorrect. (b) We add level-0 regular grid to solve the problem.

we evaluate the light field values at the vertices of the level-1 grid. In the shading stage, the light field values are sampled from the level-1 grid to shade the point samples.

As a preprocessing step, the data values on the original unstructured grid is resampled onto the level-0 regular grid. The level-0 grid covers the whole volume domain. A mask volume is also created to indicate whether a grid cell is inside the volume domain, or is a blank cell, or is inside a geometric occluder in the case that there are geometric primitives embedded in the volume. Usually we do not need a very high resolution of level-0 grid since the solution of level-0 grid only serves as the initial values of the level-1 grid in the numerical solving process.

We use the numerical method described in [26] to solve the convection equation on level-0 grid to evaluate light propagation. The resulting ρ values are interpolated onto level-1 grid as boundary conditions and the initial values for inner vertices. The convection equation is then solved on level-1 grid using a semi-Lagrangian scheme [24]. The solutions for all light sources are combined into a single light color field, and then Gauss-Seidel iteration method [9] is used to solve the diffusion step for simulating scattering effects. To shade the point samples in the rendering process, only the light color field solution on the level-1 grid is necessary. The level-0 light field can be used as a 3D texture for shading geometric primitives, which is an optional feature which enables the occlusion effects applied to the volume by the geometric primitives.

4.1 Light Volume Initialization

To initialize the level-0 light volume, we set the initial and boundary conditions according to the light settings for each light source.

For distant lights, assuming that the light direction is \mathbf{u}_D , and the energy density of the light is ρ_D , we set the initial energy density values for each vertex v in the light graph to

$$\rho(\mathbf{x}_v) = \begin{cases} \rho_D, & \text{if } \mathbf{n}(\mathbf{x}_v) \cdot \mathbf{u}_D < 0, \\ 0, & \text{otherwise} \end{cases} \quad (6)$$

where $\mathbf{n}(\mathbf{x}_v)$ is the unit outward normal at v , for boundary vertices, and set the initial values to zeros for interior vertices. As the level-0 grid is a regular grid, this process is especially simple because every vertex in the same face of the boundary box has the same initial value setting.

For point lights, assume \mathbf{x}_P is the position of the light source. If \mathbf{x}_P is outside the volume region, interior vertices are initialized to zeros, while the boundary vertices are initialized using

$$\rho(\mathbf{x}_v) = \begin{cases} G(\mathbf{x}_v, \mathbf{x}_P)\rho_P, & \text{if } \mathbf{n}(\mathbf{x}_v) \cdot (\mathbf{x}_v - \mathbf{x}_P) < 0, \\ 0, & \text{otherwise} \end{cases} \quad (7)$$

where $G(\mathbf{x}, \mathbf{x}_P)$ is the falloff function for the point light source. We use a Gaussian function for G in our implementation. If \mathbf{x}_P lies inside the volume region, the initial values are set to

$$\rho(\mathbf{x}_v) = \begin{cases} G(\mathbf{x}_v, \mathbf{x}_P), & \text{if } |\mathbf{x}_v - \mathbf{x}_P| < r_P, \\ 0, & \text{otherwise.} \end{cases} \quad (8)$$

r_P is a distance value that can be set according to the cell size of the regular grid to ensure there exists some vertices initialized to non-zero values due to the light source. In our implementation, we set r_P to twice the cell size.

4.2 Light Propagation

To simulate light propagation on the level-0 grid, we use the first-order upwind scheme presented in [26] to numerically solve Eq. 4. The result values are then interpolated onto the level-1 grid as initial and boundary conditions. Although high-order interpolation method can improve the quality, we use typical tetrahedral barycentric interpolation due to efficiency.

Our first trial to solve Eq. 4 on the level-1 grid is to apply the same scheme to the unstructured level-1 grid, but we found the method suffers from the stability problem. In the upwind scheme used for the regular grid, the time step Δt must be set to a value small enough relatively to the discretization grid size (the CFL condition) in order to achieve stable results. However, in an unstructured grid, the distance between two vertices can be very small since the interesting area is likely to be represented by denser cells. To achieve numerical stability, the Δt must be chosen according to the size of the finest cell of the mesh, which is not practical because using a small time step means a large amount of steps are needed to achieve convergence.

In order to avoid the stability problem, we use a semi-Lagrangian scheme [24], which allows larger time step while maintaining numerical stability, to solve Eq. 4 for unstructured meshes. Since the light speed and direction are constant along the particle trajectory (for both directional and point lights), for the propagation part of Eq. 4, we have the solution for the energy density at time t_{n+1} :

$$\rho_{n+1}(\mathbf{x}) = \rho_n(\mathbf{x}_d) \quad (9)$$

where the energy density at the departure point $\rho_n(\mathbf{x}_d) = \rho_n(\mathbf{x} - c\mathbf{u}\Delta t)$ can be evaluated by interpolation. And then we take absorption into account:

$$\rho_{n+1}(\mathbf{x}) = \rho_n(\mathbf{x}_d) e^{-\int_c^{\mathbf{x}} \sigma_a(s) ds} \quad (10)$$

where $\sigma_a(s)$ is the absorption coefficient at point s , and the integral is taken along the trajectory from \mathbf{x}_d to \mathbf{x} .

For a tetrahedral mesh, a typical tetrahedral interpolation method can be used to evaluate the $\rho(\mathbf{x}_d)$ value in Eq. 10. Since some cells can be very small, the step between \mathbf{x} and \mathbf{x}_d is possible to cross multiple cells, and therefore a cell traversal procedure similar to ray casting is required. The time step Δt should be small enough so that important features are not likely to be bypassed.

The calculation of Eq. 10 for each vertex can be fully parallelized, so it is suitable for a GPU implementation. Eq. 10 is iteratively applied to each vertex until a steady state solution is obtained.

Pre-integration.

4.3 Scattering

Before solving Eq. 5 for approximating scattering effects, the solutions of Eq. 4 for all light sources on level-1 grid are combined into a single light color field simply by

$$L(\mathbf{x}) = \sum_{k=1}^N \rho_k(\mathbf{x}) L_k \quad (11)$$

where ρ_k is the solution of Eq. 4 for the k th light source, and L_k is the color of the k th light source, so that we only need to solve a single diffusion equation (Eq. 5) even for multiple light sources. Therefore, Eq. 5 is modified to a vector form

$$\frac{\partial}{\partial t} L(\mathbf{x}) = \hat{\sigma}_s \nabla^2 L(\mathbf{x}) \quad (12)$$

where $\hat{\sigma}_s$ consists of three scattering coefficients for different color channels. We approximate the Laplacian of light color field at vertex v on the level-1 grid by

$$\nabla^2 L(\mathbf{x}_v) \approx \sum_{i \in N(v)} w_i (L(\mathbf{x}_i) - L(\mathbf{x}_v)) \quad (13)$$

where $N(v)$ is the neighborhood of v , and w_i is the weighting factor of neighbor i , which is inversely proportional to the square of the distance between vertices i and v , so that a closer neighbor has higher weight.

Thus, using Gauss-Seidel iteration method [9] to solve Eq. 12, in each iteration we apply

$$L(\mathbf{x}_v) \leftarrow \frac{L(\mathbf{x}_v) + \Delta t \hat{\sigma}_s \sum_{i \in N(v)} w_i L(\mathbf{x}_i)}{1 + \Delta t \hat{\sigma}_s \sum_{i \in N(v)} w_i} \quad (14)$$

to each vertex. We let $\tilde{\sigma}_s = \Delta t \hat{\sigma}_s$ be a user-defined value so that the user can determine the scattering strength.

5 IMPLEMENTATION

Our rendering system enables user to edit the transfer function and light settings interactively. Once the transfer function is changed, the opacity values at the vertices of the light graph are classified based on the transfer function. In addition, geometric primitives embedded in the volume can also act as shadow casters by setting the opacity values of the voxels of the level-0 grid associated with the geometric objects accordingly. Then for each light source, if the opacity volume or the light itself is changed, the convection result of the light must be updated. In this step, Eq. 6-8 are used for light volume initialization, and Eq. 10 is used iteratively to simulate light propagation and absorption. After the changed light volumes are updated, all light volumes are merged by Eq. 2 into a single light color field. Then we apply Eq. 14 iteratively to simulate light scattering, resulting the final illumination volume. Finally, in the rendering step, the illumination value at the sample point is interpolated as other attributes of the vertices, and the Phong shading light color is multiplied by the illumination value to shade the material during the volume rendering integral evaluation. Algorithm. 1 summarizes the procedure.

We use NVIDIA CUDA to implement the light simulation, and volume rendering is done by combined CUDA and OpenGL. The transfer function, light graph, and all per vertex values are kept in the GPU memory. The per vertex calculation including opacity classification, propagation and absorption simulation, light volume combination, and scattering simulation are all done in GPU kernels parallelly.

Ray casting method is used for volume rendering in our system. We implemented a tetrahedral ray caster similar to the one presented by Weiler et al. [25]. However, [25] and our implementation are different in that they use convexification to solve re-entry problem while we use depth peeling to deal with both re-entry and embedded geometry. The grids containing variant types of cells (pyramids, prisms, and hexahedra) are divided into tetrahedra first and rendered by ray casting as ordinary tetrahedral meshes. The illumination framework can also work with different unstructured-grid volume rendering techniques such as cell projection methods.

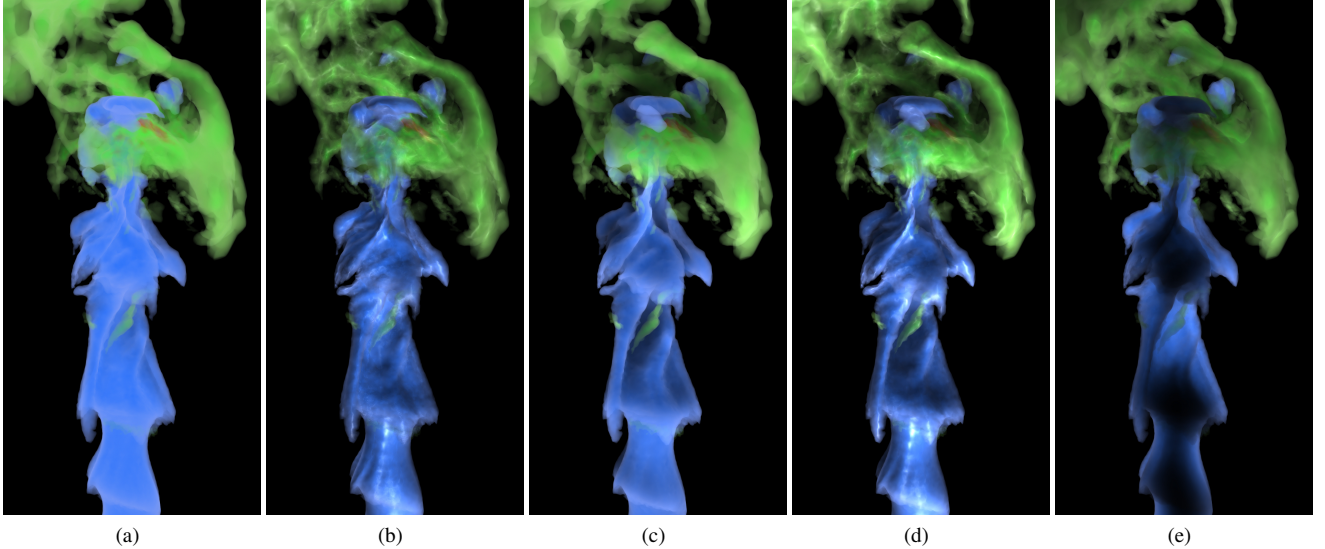


Figure 3: Comparison between different optical models. (a) The standard emission-absorption model. (b) The gradient-based Phong shading model. (c) Our advanced lighting method. (d) Our method combined with the gradient-based Phong shading. (e) Our method using a back light.

Algorithm 1 Unstructured grid-based volume illumination

```

1: for each frame do
2:   if transfer function is changed then
3:     update the opacity volume;
4:     mark all lights as changed;
5:   end if
6:   for each light source do
7:     if the light is changed then
8:       initialize the light volume;
9:       simulate light propagation and absorption;
10:    end if
11:   end for
12:   if any light changed then
13:     combine the light volumes;
14:     simulate light scattering;
15:   end if
16:   render the frame using ray casting;
17: end for

```

6 RESULTS AND DISCUSSION

Figure 1 shows the volume rendering of the H_2O field of the Flame dataset with different optical models. Figure 3 shows a closer view with a different transfer function setting. The standard emission-absorption model (Fig. 1(a) and 3(a)) provides very few information about the surface shape and depth cue. With the Lambertian diffuse and specular reflectance, the gradient-based Phong shading better reveals the surface shape (Fig. 1(b) and 3(b)). But the Phong shading model is still insufficient to resolve curtain ambiguities such as the local shape at the center region of the blue material in Fig. 3(b). With our advanced lighting method, the local darkness at the center region of Fig. 3(c) implies that this region is deeper than the vicinity so that one can clearly see the concave shape. In order to gain even more details about the local surface shape, our method can be combined with the gradient-based Phong shading (Fig. 1(c) and 3(d)). Material thickness is also one of the important aspects of volume visualization. Using a strong back light, we can get the sense of material thickness since more portion of back light is occluded as the material is thicker.

To evaluate the usefulness of our two-level approach, we tested

to apply the light simulation on level-0 grid only, and compared the result with the full level-0 + level-1 simulation as shown in Figure 4, where the velocity magnitude of the highly adaptive Aircraft1 dataset is visualized. Although the resulting images are roughly the same, the level-0-only simulation cannot accurately capture the lighting effects at the fine regions of the dataset. Increasing the resolution of level-0 grid may solve the problem, but in order to resolve the finest regions of a highly adaptive unstructured grid, a very high resolution of level-0 grid may be required, and therefore the computational cost and memory consumption may be not reasonable. The approaches that rely on the regularity of the grid (such as [1] [7] [18] [21] and [26]) may suffer from the similar problem when they are applied to unstructured data.

In our approach, we let user to select the value of $\tilde{\sigma}_a$ and $\tilde{\sigma}_s$. $\tilde{\sigma}_a$ determines the overall absorption level, while $\tilde{\sigma}_s$ determines the strength of scattering within the media. We rendered images with different $\tilde{\sigma}_a$ and $\tilde{\sigma}_s$ values to show how these parameters affect the visual appearance of the material. In Figure 5(a) and (b), the rendering results with different $\tilde{\sigma}_a$ values are compared. Obviously, with higher $\tilde{\sigma}_a$ value, the occluded regions are darker. The user can adjust this value to control the overall brightness of the image. Figure 5(c) shows that we can use high $\tilde{\sigma}_a$ value with high light intensity (ρ_D or ρ_P) to create an image with high contrast. The images with different $\tilde{\sigma}_s$ values are compared in Figure 6 ($\tilde{\sigma}_s = 0.1$ in (a) and $\tilde{\sigma}_s = 10$ in (b)). Two directional light sources are used: a blue light on the left side and an orange back light. With stronger scattering, Fig. 6(b) is slightly brighter, and the different light colors are blended more, especially at the boundary where the light from the back light can scatter through the material. Also, the shadows in Fig. 6(b) are softer; we can adjust the $\tilde{\sigma}_s$ value to control the softness of the shadows.

6.1 Performance

We tested our method on an NVIDIA GeForce GTX Titan graphics card with 6 GB of video memory, installed on a PC with an Intel Core i7 3.5 GHz processor and 32 GB of main memory. Table 1 shows the characteristics of the datasets as well as the performance measurements; the timing numbers of the propagation calculation and the scattering calculation for level-0 and level-1 grid are listed respectively. The total processing times, the summation of above numbers, are also given in the table. In all test cases, a

Table 1: Performance measurements for the datasets of this paper. The light volume calculation times are measured using a single directional light source. The resolution of level-0 grid is $128 \times 128 \times 128$.

Dataset	#Vertices	#Tetrahedra	Level-0 Propagation	Level-0 Scattering	Level-1 Propagation	Level-1 Scattering	Total
Aircraft1	103 K	567 K	73 ms	12 ms	6 ms	20 ms	111 ms
Aircraft2	165 K	935 K	58 ms	11 ms	6 ms	24 ms	99 ms
Aircraft3	804 K	4.6 M	53 ms	10 ms	25 ms	136 ms	224 ms
Flame	538 K	3.2 M	57 ms	10 ms	15 ms	88 ms	170 ms
Engine	1.2 M	6.0 M	64 ms	11 ms	28 ms	152 ms	255 ms
Train	1.0 M	6.1 M	60 ms	11 ms	19 ms	123 ms	213 ms
Car	4.2 M	24.7 M	56 ms	11 ms	126 ms	561 ms	754 ms

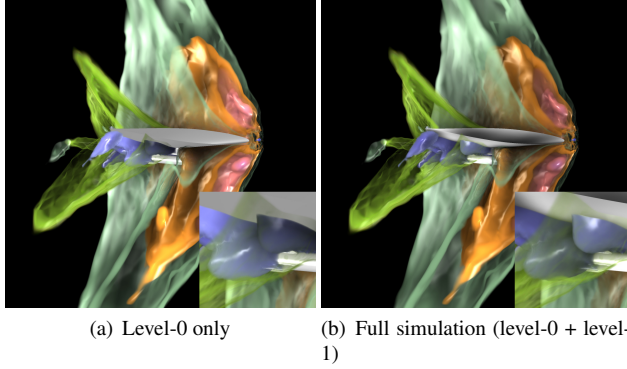


Figure 4: Simulating the light only on the level-0 grid cannot accurately capture the lighting effects at the fine regions of a highly adaptive grid.

single directional light source is used. When multiple light sources are used, the propagation calculation is performed for each light source, while the scattering calculation is needed to be done only once. The overall processing takes several hundred milliseconds in our test cases, which is almost achieve interactive requirement. With our implementation, the light volume calculation time is usually even shorter than the rendering time (using ray casting) when the image size is over 1024×1024 . Also notice that the light simulation is view-independent and is not necessarily computed for every frame. Instead, only when the transfer function or the light setting is changed, the light volume is needed to be updated. And since our propagation and scattering computation is iterative, the computation burden can be separated to multiple frames in order to improve the interactivity of the rendering system.

The resolution of level-0 grid used in Table 1 is $128 \times 128 \times 128$, which is sufficient to generate acceptable results in our test cases. The computational cost for level-0 grid is dependent upon the resampling resolution. We tested different resolutions and the timing results are similar to the results of [26]. Interested readers are referred to [26].

On the level-1 grid, the light propagation and scattering calculation is applied at the vertices of the grid. Therefore, the computational cost should be linearly proportional to the grid size. For scattering, the computation takes place between a vertex and each adjacent vertex of it, so the degree of the vertices also effects the cost. However, the degree of vertices does not increase with the data size and usually can be seen as constant. In order to verify our time complexity estimation, we applied the method to a set of synthesized grids. We resampled the Vortex regular-grid dataset onto tetrahedral grids of different sizes (from 500K to 30M). The calculation times of propagation and scattering on level-1 grids are shown in Figure 7. It can be clearly seen that both propagation and

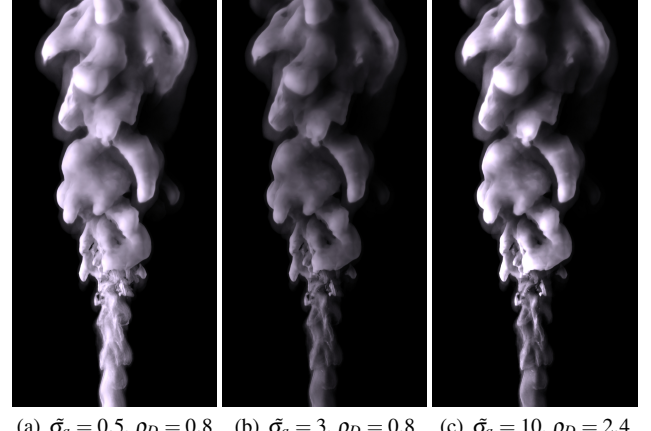


Figure 5: Rendering results with different absorption coefficient σ_a . As σ_a increases, the shadows become darker.

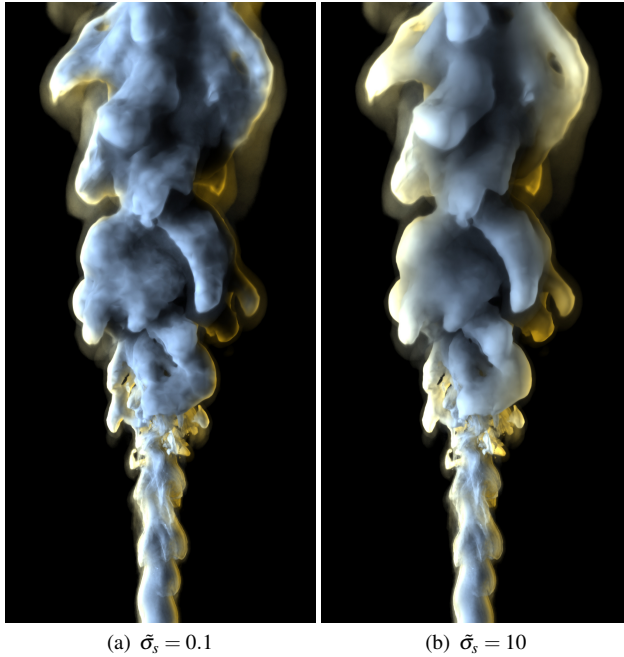
scattering times are about linearly proportional to the grid size. And the total calculation time for the largest grid we tested is still under one second.

In the rendering stage, for each sample point, additional few memory fetches are needed to sample the light volume in order to apply our illumination technique. We measured the rendering time for a single frame with and without enabling our illumination method, respectively, to evaluate the impact of the technique to the rendering performance. The experimental results show that the impact is insignificant; When enabling the advanced illumination effects, the rendering time only increases slightly (under 10% in all tested datasets) comparing to the rendering time without the effects.

In order to speed up, Zhang and Ma [26] downsamples light volumes for light simulation and argues that usually a light volume with half resolution of original volume data is able to produce visually plausible results. In our scheme, the resolution of level-0 grid is user-adjustable and it can be chosen to trade visual quality for performance. For level-1 grid, an unstructured grid simplification method such as [4] or [5] can be used to generate simplified grid for light simulation.

7 CONCLUSION AND FUTURE WORK

We have presented an illumination method optimized for volume visualization of unstructured-grid data, which uses a two-level light volume calculation scheme. Firstly, a rough but fast light simulation is performed on the level-0 grid, a regular grid resampled from the original data. And then the light simulation on the unstructured level-1 grid is performed to provide detailed lighting effects. The lighting calculation on the level-1 grid uses a novel numerical scheme that is fully GPU accelerated to solve the model equa-

Figure 6: Rendering results with different scattering coefficient $\bar{\sigma}_s$.

tion. The added global shadowing and multiple scattering effects enhance depth cues and perception of complex spatial relationships for volume visualization. Test results show that the performance of our method is sufficient for interactive volume exploration.

Our method does not rely on heavy precomputation. The only necessary precomputation for the method is the resampling for the level-0 grid. Comparing to other essential precomputation tasks such as gradient estimation used for gradient-based Phong shading, the preprocessing time for our method is even ignorable. This makes it possible to be used for time-varying data visualization.

It is not hard to extend our method to support other types of grids including curvilinear grids, adaptive mesh refinement (AMR) grids, and even hybrid grids. Under our framework, the level-1 grid can be replaced by the desired grid type. For AMR grids, a multi-level scheme can be used to fit the grid resolution.

In the future, we would like to support illumination of large-

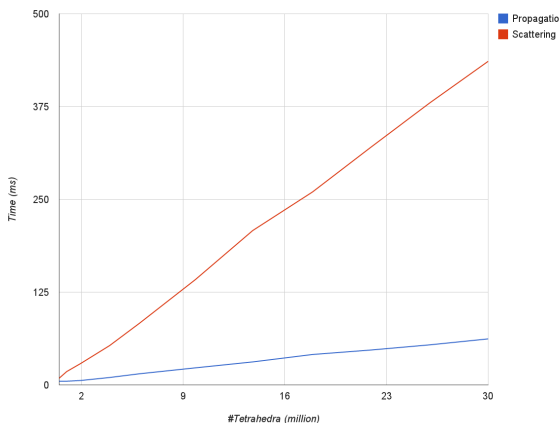


Figure 7: Level-1 grid calculation times for different data sizes.

scale, time-varying unstructured grid data. Thanks to the parallel nature of our technique, it is straightforward to implement the algorithm on multi-GPU machines or GPU clusters. Also, as mentioned in Section 6.4, we would like to support level-of-detail to facilitate interactivity for visualization of large datasets. Another topic of future research would be the anisotropic scattering of light, which provides more realistic appearances of materials while our current illumination model considers only isotropic scattering.

REFERENCES

- [1] M. Ament, F. Sadlo, and D. Weiskopf. Ambient volume scattering. *Visualization and Computer Graphics, IEEE Transactions on*, 19(12):2936–2945, Dec 2013.
- [2] A. Boudet, P. Pitot, D. Pratmarty, and M. Paulin. Photon splatting for participating media. In *Proc. of GRAPHITE*, pages 197–204, 2005.
- [3] S. Chandrasekhar. *Radiative Transfer*. Dover Publications, New York, 1960.
- [4] P. Choppa and J. Meyer. Tefusion: an algorithm for rapid tetrahedral mesh simplification. In *Visualization, 2002. VIS 2002. IEEE*, pages 133–140, Nov 2002.
- [5] P. Cignoni, D. Costanza, C. Montani, C. Rocchini, and R. Scopigno. Simplification of tetrahedral meshes with accurate error evaluation. In *Visualization 2000. Proceedings*, pages 85–92, Oct 2000.
- [6] C. D. Correa, R. Hero, and K.-L. Ma. A comparison of gradient estimation methods for volume rendering on unstructured meshes. *IEEE Transactions on Visualization and Computer Graphics*, 17(3):305–319, May 2011.
- [7] J. Díaz, P. Vázquez, I. Navazo, and F. Duguet. Real-time ambient occlusion and halos with summed area tables. *Computers & Graphics*, 34(4):337–350, 2010.
- [8] W. Jarosz, M. Zwicker, and H. W. Jensen. The beam radiance estimate for volumetric photon mapping. *Computer Graphics Forum*, 27(2):557–566, 4 2008.
- [9] S. Jeffreys and B. Jeffreys. *Methods of mathematical physics*. Cambridge University Press, 1966.
- [10] H. W. Jensen and P. H. Christensen. Efficient simulation of light transport in scenes with participating media using photon maps. In *Proc. of SIGGRAPH*, pages 311–320. ACM, 1998.
- [11] D. Jonsson, J. Kronander, T. Ropinski, and A. Ynnerman. Historygrams: Enabling interactive global illumination in direct volume rendering using photon mapping. *Visualization and Computer Graphics, IEEE Transactions on*, 18(12):2364–2371, Dec 2012.
- [12] J. T. Kajiya and B. P. Von Herzen. Ray tracing volume densities. In *Proceedings of the 11th annual conference on Computer graphics and interactive techniques, SIGGRAPH '84*, pages 165–174, New York, NY, USA, 1984. ACM.
- [13] J. Kniss, S. Prempoze, C. Hansen, and D. Ebert. Interactive translucent volume rendering and procedural modeling. In *Visualization, 2002. VIS 2002. IEEE*, pages 109–116, Nov 2002.
- [14] J. Kniss, S. premoze, C. Hansen, P. Shirley, and A. McPherson. A model for volume lighting and modeling. *Visualization and Computer Graphics, IEEE Transactions on*, 9(2):150–162, 2003.
- [15] E. P. Lafourche and Y. D. Willems. Rendering participating media with bidirectional path tracing. In *Proc. of EGWR*, pages 91–100, 1996.
- [16] M. Levoy. Efficient ray tracing of volume data. *ACM Trans. Graph.*, 9(3):245–261, July 1990.
- [17] N. Max. Optical models for direct volume rendering. *IEEE Transactions on Visualization and Computer Graphics*, 1(2):99–108, June 1995.
- [18] T. Ropinski, C. Döring, and C. Rezk-Salama. Interactive volumetric lighting simulating scattering and shadowing. In *PacificVis*, pages 169–176, 2010.
- [19] M. Ruiz, I. Boada, I. Viola, S. Bruckner, M. Feixas, and M. Sbert. Obscurrence-based volume rendering framework. In *Proceedings of Volume Graphics 2008*, pages 113–120, Aug. 2008.
- [20] H. E. Rushmeier and K. E. Torrance. The zonal method for calculating light intensities in the presence of a participating medium. *SIGGRAPH Comput. Graph.*, 21:293–302, 1987.

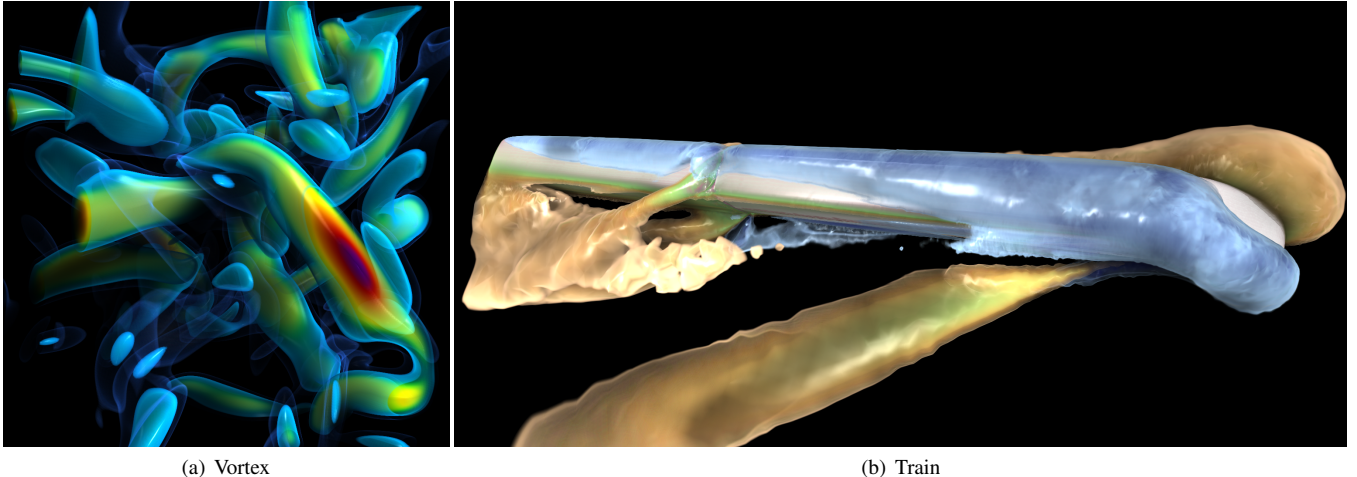


Figure 8: Rendering examples using our method.

- [21] P. Schlegel, M. Makhinya, and R. Pajarola. Extinction-based shading and illumination in gpu volume ray-casting. *Visualization and Computer Graphics, IEEE Transactions on*, 17(12):1795–1802, Dec. 2011.
- [22] M. Schott, T. Martin, A. Grossset, S. Smith, and C. Hansen. Ambient occlusion effects for combined volumes and tubular geometry. *Visualization and Computer Graphics, IEEE Transactions on*, 19(6):913–926, 2013.
- [23] P. Shanmugam and O. Arikán. Hardware accelerated ambient occlusion techniques on gpus. In *Proc. of I3D*, pages 73–80, 2007.
- [24] C. Smith and U. of Reading. *The Semi Lagrangian Method in Atmospheric Modelling*. 2000.
- [25] M. Weiler, M. Kraus, M. Merz, and T. Ertl. Hardware-based ray casting for tetrahedral meshes. In *Proceedings of the 14th IEEE Visualization 2003 (VIS'03)*, VIS '03, pages 44–, Washington, DC, USA, 2003. IEEE Computer Society.
- [26] Y. Zhang and K.-L. Ma. Fast global illumination for interactive volume visualization. In *Proceedings of the ACM SIGGRAPH Symposium on Interactive 3D Graphics and Games*, I3D '13, pages 55–62, New York, NY, USA, 2013. ACM.